plant biology

Plant Biology ISSN 1435-8603

RESEARCH ARTICLE

Surviving adversity: Exploring the presence of *Lunularia cruciata* (L.) Dum. on metal-polluted mining waste

A. De Agostini[1], P. Cortis[1], F. S. Robustelli della Cuna[2], F. Soddu[3], C. Sottani[2], D. N. Tangredi[4,5], F. Guarino[4,5], A. Cogoni[1], A. Vacca[6] & C. Sanna[1]

1 Department of Life and Environmental Sciences, University of Cagliari, Cagliari, Italy
2 Environmental Research Center, Istituti Clinici Scientifici Maugeri IRCCS, Pavia, Italy
3 Neuroimmunology Laboratory, IRCCS Mondino Foundation, Pavia, Italy
4 Department of Chemistry and Biology "A. Zambelli", University of Salerno, Fisciano, Italy
5 NBFC National Biodiversity Future Center, Palermo, Italy
6 Department of Chemical and Geological Sciences, University of Cagliari, Monserrato, Italy

Keywords
Bryophytes; clorophyll fluorescence; extreme environments; heavy metals; liverworts; sesquiterpenes; volatile organic compounds.

Correspondence
P. Cortis, Department of Life and Environmental Sciences, University of Cagliari, Via S. Ignazio da Laconi 13, Cagliari 09123, Italy.
E-mail: pierluigi.cortis@unica.it

Editor
F. Loreto

Received: 22 March 2024;
Accepted: 9 June 2024

doi:10.1111/plb.13686

ABSTRACT

- The tailings dump of Barraxiutta (Sardinia, Italy) contains considerable concentrations of heavy metals and, consequently, is scarcely colonized by plants. However, wild populations of the liverwort *Lunularia cruciata* (L.) Dum. form dense and healthy-looking carpets on this tailing dump.
- *L. cruciata* colonizing the tailing dump was compared with a control population growing in a pristine environment in terms of: (i) pollutant content, (ii) photochemical efficiency, and (iii) volatile secondary metabolites in thalli extracts.
- *L. cruciata* maintained optimal photosynthesis despite containing considerable amounts of soil pollutants in its thalli and had higher sesquiterpene content compared to control plants.
- Sesquiterpenes have a role in plant stress resistance and adaptation to adverse environments. In the present study, we propose enhanced sesquiterpenes featuring Contaminated *L. cruciata* as a defence strategy implemented in the post-mining environment.

INTRODUCTION

Mining activity for extraction of materials from the Earth's crust has accompanied human civilisations since their origin. Past mining, however, has left a legacy of byproducts of extractive processes which are still today contaminated by inorganic pollutants, especially heavy metals. Besides the threat these pose to human health (Varrica *et al.* 2014; Beane *et al.* 2016; Rodríguez-Eugenio *et al.* 2018; De Giudici *et al.* 2019), metalliferous environments (*i.e.*, environments containing single or multiple metallic or semi-metallic elements) are restrictive habitats for plants. In fact, phytotoxic metals or supra-optimal levels of essential metals cause abiotic stress, defined as "heavy metal stress", which adversely affects plant and crop productivity (Singh *et al.* 2015). Heavy metal stress negatively affects photosynthesis, enzyme activity, nutrient uptake, embryo development, seed germination, and plant biomass production. It also generates oxidative stress through accumulation of reactive oxygen species (ROS) in cells, leading to damage to membranes and photosynthetic centres, as well as ion leakage, DNA cleavage, and ultimately, programmed cell death (Vickers *et al.* 2009; Rascio & Navari-Izzo 2011; Hodson 2012; Singh *et al.* 2015). However, the selective pressure in metalliferous environments may lead to the speciation of plant *taxa* or ecotypes that can thrive (metal-tolerant) or are only found (metallophytes) in environments far too toxic for non-adapted plants (Baker *et al.* 2010).

Among the defences and adaptive strategies that plants may put in place in response to adverse environments, such as metalliferous environments, the production of specialized metabolites is one of the most ancient and conserved (Loreto *et al.* 2014b; Liang *et al.* 2018). Emission of volatile secondary metabolites, such as isoprenoids, alkanes, alkenes, carbonyls, alcohols, esters, ethers, and acids, known as biogenic volatile organic compounds (BVOCs) (Kesselmeier & Staudt 1999), is the basis of crucial ecological interactions and plays a role in stress resistance and adaptation to extreme environments (Peñuelas & Llusià 2004; Rinnan *et al.* 2014; Loreto *et al.* 2014a).

The present study focused on the liverwort *Lunularia cruciata* (L.) Dum. Liverworts, mosses and hornworts are bryophytes, and close relatives of the first plants that abandoned water around 470–515 million years ago (Chen *et al.* 2018b; Li *et al.* 2020). Bryophytes are still excellent early land colonizers which in some cases are able to thrive on extreme and severely polluted environments that are unavailable for most vascular plants (Karakaya *et al.* 2015; De Agostini *et al.* 2022; Degola *et al.* 2022; Campbell *et al.* 2023). The current investigation centers on the presence of the liverwort *L. cruciata* in the Barraxiutta tailings dump in Sardinia (Italy), which is characterized by severe soil pollution from mining activities. The

objective of the present study was to understand how *L. cruciata* can thrive in such adverse conditions. To accomplish this, plants were initially analysed for pollutant content to determine whether they exclude or take up soil pollutants. Subsequently, since photosynthesis is one of the first processes negatively affected by heavy metal stress, the Normalized Difference Vegetation Index (NDVI) and chlorophyll fluorescence parameters were calculated to evaluate plant health and effects of phytotoxic elements on photosynthesis. Finally, to explore potential secondary metabolites-based defence mechanisms employed by *L. cruciata* to mitigate soil phytotoxicity, a comprehensive analysis of volatile organic compounds in plant extracts was conducted, identifying and characterizing individual components and relating them to soil pollution. We postulated that volatile isoprenoids (VIs), especially sesquiterpenes, might serve as crucial elements in the adaptive strategies of this species to the harsh conditions of the study site.

MATERIALS AND METHODS

Study site

The tailing dump of "Barraxiutta" (39°22′5.82″ N, 8°36′28.46″ E – WGS84), Contaminated site hereafter, is in the abandoned mining district of "Sa Duchessa" in the municipality of Domusnovas (Sardinia, Italy). Mining activity in the district ended in the second half of the twentieth century. Lead (Pb) and zinc (Zn) were extracted from Sphalerite and Galena through underground mining and processed *in situ*. Consequently, the tailings dump exhibits significant contamination with heavy metals, especially of Fe, Zn, and Pb, as previously documented by our team (De Agostini *et al.* 2020a, 2020b).

An uncontaminated site, Control site hereafter, hosting the control population of *L. cruciata* was chosen in the municipality of Sinnai (39°18′9.30″ N, 9°23′52.85″ E – WGS84), more precisely in the regional park "Sette Fratelli". This site was chosen for the absence of any anthropic activity that could have originated or dispersed pollutants and for its similar environmental conditions as the tailing dump (i.e., shady Mediterranean *Quercus* sp. forest).

Substratum collection and analysis

Soil features of control and contaminated sites were characterized following standard procedures outlined in Schoeneberger *et al.* (2012) on the topsoil (0–25 cm). The collected bulk soil samples (three replicates per study site) were air-dried and crushed to a particle size of 2 mm. Subsequently, sand (2.00–0.05 mm), silt (0.05–0.002 mm), and clay (<0.002 mm) fractions were separated by sieving and pipetting following organic matter removal with H_2O_2 and dispersion with Na-hexametaphosphate. The organic carbon (C) content was quantified using a C elemental analyser (Leco, USA). Total nitrogen (N) was assessed through the Kjeldahl method, while total phosphorus (P) was determined via spectrophotometry subsequent to treatment with H_2SO_4, H_2O_2, and HF. Available P was analysed using the Olsen method, total K was determined via spectrophotometry following treatment with H_2SO_4, HCl, and HF, and available K was assessed through spectrophotometry after treatment with HCl and $BaCl_2$. Soil pH was measured potentiometrically in soil/solution suspensions of 1.0:2.5 H_2O. Sieved samples were subjected to digestion in concentrated HNO_3 according to EPA 3050-B method for determination of total metal content (Fe, As, Cd, Cu, Cr, Pb, Zn, Ni, Mn). The bioavailable fractions of metals were determined utilizing the Community Bureau of Reference (BCR) extraction method (0.11 M acetic acid). The resulting soil extracts were analysed using Inductively Coupled Plasma (ICP-OES 5110; Agilent, USA).

Plant material

Thalli of the liverwort *L. cruciata* (Marchantiophyta; Lunulariaceae H. Klinggr.) are 2.5-cm long, 5–10-mm wide, irregularly and dichotomously branched. The monospecific genus *Lunularia* is named after the distinctive semilunar gemmae cups containing the lenticular gemmae for asexual propagation. *L. cruciata* grows on damp soils, rocks, walls, and paths in natural and manmade environments at low altitudes (Smith 1990). Healthy-looking green thalli of *L. cruciata* were collected for determination of element content and for BVOC extraction from the Contaminated and Control sites. Plant material (Figure S1) was sampled in the first week of May 2021 in the Control and Contaminated sites to avoid differences in the chemical profiles attributable to seasonality. Thalli were collected across the study sites (on soils with uniform pedological features), sampling portions of carpets until reaching a total area of approximately 50 × 50 cm per growing condition, each hosting tens of individuals. This approach was chosen to ensure that the sampling was both spatially adequate and representative of the population intra-variability (while paying attention to preservation of the natural populations). Plant material was first washed of any debris with distilled water in an ultrasonic bath (Ultrasonic cleaner model 1210; Bransonic, USA), and then weighed (AE260 Analytical Balance; Mettler, USA) to obtain the fresh weight (FW).

Element content

A portion of plant material for each site was air-dried to constant weight for measurement of the content of Al, Ca, Cd, Co, Cr, Cu, Fe, K, Mg, Na, Ni, P, Pb, S, Si and Zn. Briefly, 125 mg dry weight (DW) per growing condition, corresponding to ca 3 individuals, was ground in liquid nitrogen and digested in 65% nitric acid (HNO_3) and 50% hydrofluoric acid (HF), 2:1 ratio (v/v). Digestion took place in a microwave oven (Ethos, Milestone, Italy). The element concentrations in plant thalli were determined using Inductively Coupled Plasma–Optical Emission Spectrometry analysis (ICP–OES) (Optima 7000DV; PerkinElmer, USA) and obtained data compared to standard references to verify accuracy of the analysis (Thomas 2003). Standard solutions were used to generate calibration curves of emission reading vs concentration for each element. Analyses were performed in triplicate.

Normalized difference vegetation index

The Normalized Difference Vegetation Index (NDVI) indicates plant health and vigour based on plant reflective properties. Plants absorb red light (harvested by chlorophylls and accessory pigments) but reflect near infrared light. NDVI is then calculated from the formula

$$\frac{(\%\text{reflected near infrared light} - \%\text{reflected red light})}{(\%\text{reflected near infrared light} + \%\text{reflected red light})} \quad (1)$$

NDVI values range from −1 to +1: NDVI values from −1 to 0 indicate dead plants, while values from 0 to 1 indicate increasingly healthy and vigorous plants. In the present study, NDVI was measured using the Fieldscout CM 1000 NDVI Meter (Spectrum Technologies, USA), with the instrument held ca 50 cm above *L. cruciata* carpets in both Contaminated and Control sites. NDVI values discussed here are the average of 10 repeated measurements on different carpet portions.

Chlorophyll fluorescence parameters

In vivo chlorophyll fluorescence assays are used to investigate the toxicity and mode of action of phytotoxic elements to assess photosynthesis and physiological status (Mallick & Mohn 2003; Velikova *et al.* 2011). Fluorescence parameters were measured with a Mini PPM 100 fluorometer (EARS, Netherlands) on 1 h dark-adapted plants. The instrument measured within 1s, minimum fluorescence (F_0) (using non-actinic measuring flashes) and maximum fluorescence (F_m) after a saturating light pulse (8000 μmol·photon·m^{-2}·s^{-1}). The following fluorescence parameters were considered as indicators of heavy metal phytotoxicity affecting photosynthesis (Mallick & Mohn 2003; Velikova *et al.* 2011): F_0; F_m; variable fluorescence F_v ($F_v = F_m - F_0$); maximum quantum yield of photosystem II (F_v/F_m); plastoquinone pool ($F_v/2$); and F_0/F_v ratio as an indicator of efficiency of water-splitting. Fluorescence measurements were carried out on *L. cruciata* growing in the Contaminated (n = 15) and Control (n = 10) sites.

Extraction of BVOC

Frozen thalli from Contaminated (18.3 g FW) and Control (8.16 g FW) sites, corresponding, respectively, to ca. 70 and 40 individuals, were used for BVOC extraction. Octyl octanoate (0.25 mg) was added to plant material as an internal standard, and steam distilled for 3 h with distilled water according to Robustelli della Cuna *et al.* (2019) with slight modifications. Diethyl ether (100 ml) was used to separate the organic and aqueous phases through three repeated liquid/liquid extractions. The obtained organic phase was completely dehydrated using anhydrous sodium sulphate and then rotary evaporated. The yield of the extracts is the ratio between the extract weight (g) and the plant material FW (g). Extracts were kept at −20 °C until GC/FID and GC/MS analyses.

Analysis with GC-FID and GC-Ms

Analyses (three replicates) of extract components were carried out using a Hewlett Packard model 5980 GC, equipped with Elite-5MS (5% phenyl methyl polysiloxane) capillary column (30 m × 0.32 mm i.d.) with film thickness 0.32 μm. Helium was carrier gas at 1 ml·min^{-1}. Before analysis, samples were diluted in diethyl ether (1 μg·ml^{-1}), and 1 μl was manually injected in split mode (30:1). The oven temperature program was initial isotherm of 40 °C (5 min), followed by a temperature ramp to 260 °C at 4 °C·min^{-1}, maintained as a final isotherm (10 min). Injector and detector temperatures were set at 250 and 280 °C, respectively. The relative amount of each component was calculated considering the corresponding FID peak area without response factor correction. The GC-MS analyses were carried out with a GC Model 6890 N, coupled to a benchtop MS Agilent 5973 Network, equipped with the same capillary column as above and following the same GC/FID analyses chromatographic conditions. Helium was the carrier gas at 1.0 mL·min^{-1}. Ion source temperature was set at 200 °C, while the transfer line was at 300 °C. Acquisition range was 40–500 amu in electron-impact (EI) positive ionization mode, ionization voltage of 70 eV (Robustelli della Cuna *et al.* 2022). Octyl octanoate (98%), alkane mix (C6–C35), and anhydrous sodium sulphate were obtained by Sigma-Aldrich (USA). Diethyl ether was purchased from Merck (Germany). Ultrapure water (LC-MS grade) was produced using Milli Q-Milli RO system, Millipore (USA).

Identification of BVOC

Volatile components in the extracts were identified by their retention indices (RI) and mass spectra and by comparison with a NIST database mass spectral library, as well as with literature data (Stein 2000; Adams 2017). The relative amount of each component was expressed as percentage peak area relative to total peak area from GC/MS analyses of whole extracts using the following equation:

$$\text{Relative content } (\%) = \left(\frac{\text{Area under peak}}{\text{Total peak area}}\right) \times 100 \quad (2)$$

Retention indices were calculated by Elite-5MS capillary columns using an n-alkane series (C_6–C_{35}) under the same GC conditions as for the samples. The retention indices (RI) were calculated as shown in equation:

$$RI = 100 \times n + \frac{[100 \times (tx - tn)]}{(tn + 1 - tn)} \quad (3)$$

where RI is retention index of the unknown compound x, n is number of C atoms of the n-alkane eluted before x, n + 1 is number of C atoms of the n-alkane eluted after x, tx is retention time of x, tn is retention time of the n-alkane eluted before x, and tn + 1 is retention time of the n-alkane eluted after x. The relative abundance of chemical classes was obtained by adding the relative abundance of the compounds forming part of each chemical class.

Statistical analysis

The statistical significance of differences in the content of elements in soil samples and *L. cruciata* thalli, as well as of fluorescence parameters was assessed by *t*-test. The assumptions necessary for its implementation were met, and corrections were applied in cases of non-homogeneous variance. When reported, effect size of observed differences was calculated with Cohen's d effect size Hedge's Corrected for small samples (n < 50). Boxplots were drawn to represent *L. cruciata* F_v/F_m in Control and Contaminated populations. To provide immediate insight to chemical composition of the extracts from the two populations of *L. cruciata*, stacked bar plots are provided. A

principal component analysis (PCA) was carried out, considering plant element content and BVOCs profiles in the two populations. PCA results are represented by a biplot, reporting both individuals and variables in the PCA space. In the biplot, variables are represented as arrows originating from the intersection between the two principal axes. Variables should be considered directly or inversely proportional whether they point the same or the opposite direction, respectively. Variables pointing towards clusters of individuals are highly representative of the features of that cluster. For the relationship between sesquiterpenes and heavy metals content in *L. cruciata* thalli, correlations between heavy metals (Cd, Cu, Fe, Pb and Zn) and sesquiterpenes (either considered together or individually) in *L. cruciata* extracts were tested with Pearson, Spearman or Kendall method (depending on data features). Correlations were considered significant at *p*-values less than the 0.05 threshold. All statistical analyses were carried out using R-software, version 4.1.3 (10 March 2022) (R Core Team 2022) implemented with the following packages: "ggpubr", "dplyr" for barplot and boxplots; "dplyr", "FactoMineR", "factoextra" for PCA; "lares" for the representation of correlations.

RESULTS

Pedological and physicochemical soil features

In the Contaminated site, the analysed topsoil (ˆA horizon) contained 89.1% sand, 8.7% silt, and 2.2% clay, was weak and very fine, had a fine subangular blocky structure with a tendency to single grains, was soft, nonsticky, nonplastic, with strong effervescence after 1 N HCl application. Organic C content of 50%, and pH (H_2O) of 8.0. Total N was $<0.1\ g{\cdot}kg^{-1}$, total P $388\ mg{\cdot}kg^{-1}$, available P $3.48\ mg{\cdot}kg^{-1}$, total K $500\ mg{\cdot}kg^{-1}$, and available K $10\ mg{\cdot}kg^{-1}$. Since the analysed topsoil was formed on material created by humans as part of a mining process (mine spoil), soil is classified as Spolic Technosols (IUSS Working Group WRB 2022).

In the Control site, the analysed topsoil (A horizon) had loam texture (51% sand, 31% silt, and 18% clay), moderate fine subangular blocky structure, soft, slightly sticky and non-plastic wet consistence and organic C 1.77% and pH (H_2O) 7.5. Total N is $1.69\ g{\cdot}kg^{-1}$, total P $137\ mg{\cdot}kg^{-1}$, available P $4.49\ mg{\cdot}kg^{-1}$, total K $1{,}768\ mg{\cdot}kg^{-1}$, and available K $102\ mg{\cdot}kg^{-1}$. Soils in the area are classified as Eutric Cambisols (IUSS Working Group WRB 2022).

The total and bioavailable concentration of heavy metals in the Control and Contaminated sites are reported in Table 1.

Heavy metal content in plant samples

Element content in *L. cruciata* samples varied markedly between the two populations. Contaminated *L. cruciata* had a significantly higher content of Ca, Cd, Cu, Fe, Pb and Zn with respect to controls. Ca should be attributed to the carbonate lithology of the Contaminated site, while Cd, Cu, Fe, Pb and Zn reflect the composition of the mining waste on which *L. cruciata* grows. Control individuals, on the contrary, presented significantly higher Al, K, Na and Si with respect to Contaminated plants, reflecting the granitoid lithology of the Control site. Element content in Contaminated and Control individuals is reported in Table 2.

Table 1. Soil metal concentrations and bioavailability at the control and contaminated sites.

			test statistics		
	control ($mg\ g^{-1}$)	contaminated ($mg\ g^{-1}$)	test statistic	df	*p*-value
Element (total)					
[Cr]	0.13 ± 0.07	0.06 ± 0.05	−1.41	4	0.23
[Mn]	0.37 ± 0.22	1.19 ± 0.81	1.7	4	0.16
[Fe]	**19.96 ± 1.67**	**63.8 ± 1.79**	**31.03**	**4**	**<0.001**
[Ni]	0.83 ± 0.61	0.22 ± 0.10	−1.71	4	0.16
[Cu]	**0.01 ± 0.01**	**0.87 ± 0.52**	**2.87**	**4**	**0.04**
[Zn]	**0.64 ± 0.42**	**14.3 ± 0.91**	**23.62**	**4**	**<0.001**
[Cd]	**0.005 ± 0.005**	**0.16 ± 0.08**	**3.18**	**4**	**0.03**
[Pb]	**0.21 ± 0.001**	**5.9 ± 1.39**	**7.06**	**4**	**0.002**
[As]	l.o.d.	0.23 ± 0.12	NA	NA	NA
Element (bioavailable)					
[Cr]	0.01 ± 0.01	l.o.d.	NA	NA	NA
[Mn]	**0.25 ± 0.24**	**2.37 ± 1.08**	**3.33**	**4**	**0.03**
[Fe]	0.83 ± 0.86	0.08 ± 0.08	− 1.50	4	0.21
[Ni]	0.03 ± 0.02	l.o.d.	NA	NA	NA
[Cu]	l.o.d.	0.07 ± 0.03	NA	NA	NA
[Zn]	**0.20 ± 0.08**	**4.9 ± 0.98**	**8.25**	**4**	**0.001**
[Cd]	**0.002 ± 0.001**	**1.01 ± 0.56**	**3.14**	**4**	**0.03**
[Pb]	**0.27 ± 0.02**	**3.48 ± 0.75**	**7.37**	**4**	**0.002**
[As]	l.o.d.	l.o.d.	NA	NA	NA

Data are expressed as mean ($mg{\cdot}g^{-1}$) ± SD of three replicates; l.o.d = Limit of Detection. The last three columns report statistical test results: bold letters indicate statistical significance of differences between the element content of Control and Contaminated soils.

Normalized difference vegetation index

The NDVI of Control and Contaminated *L. cruciata* was 0.43 and 0.42, respectively. This indicates that both Control and Contaminated plants can absorb adequate and comparable amounts of photosynthetically active light. The difference between Control and Contaminated NDVI is in fact not significant (*t*-test = −0.23, df: 16, $p = 0.81$) and the effect size is −0.11 (Cohen's d effect size Hedge's Corrected for small samples, $n < 50$). NDVI data are reported in Table S1.

Chlorophyll fluorescence parameters

In the present study the fluorescence parameters considered were F_0, F_m, F_v/F_m, $F_v/2$ and F_0/F_v (Table S2). These parameters are considered as indicating photosynthetic efficiency and diagnostic of heavy metal stress acting on photosynthetic machinery (Mallick & Mohn 2003; Bibbiani *et al.* 2018). In the present study F_0, F_m, F_v/F_m and $F_v/2$, significantly increased in Contaminated individuals with respect to Controls (Table 3), while F_0/F_v decreased in Contaminated *L. cruciata* (Table 3). In the case of F_v/F_m (Fig. 1), both Control and Contaminated values are largely within the range of values indicating optimal photosynthesis in bryophytes (López-Pozo *et al.* 2019) despite soil pollution, however physiological relevance of the measured difference (4% higher in Contaminated *L. cruciata*), should be considered negligible and unrelated to the growing conditions. This was confirmed by the absence of any significant correlation between increasing heavy metals in *L. cruciata* thalli and F_v/F_m

Table 2. Element concentration in *Lunularia cruciata* from control and contaminated populations.

			significance of differences		
element	control	contaminated	test statistic	df	*p*-value
[Al]	**201.42 ± 37.03**	**59.14 ± 9.76**	**5.17**	**4**	**0.007**
[Ca]	**28.41 ± 3.13**	**109.87 ± 25.84**	**−4.59**	**2.06**	**0.042**
[Cd]	**l.o.d.**	**0.16 ± 0.06**	**−4.33**	**2**	**0.049**
[Co]	0.12 ± 0.00	0.10 ± 0.03	1.73	2	0.225
[Cr]	0.25 ± 0.04	0.11 ± 0.04	1.63	4	0.178
[Cu]	**0.01 ± 0.01**	**1.39 ± 0.16**	**−11.49**	**2**	**0.007**
[Fe]	**43.48 ± 3.45**	**287.71 ± 46.43**	**−7.22**	**2.02**	**0.018**
[K]	**108.26 ± 1.10**	**55.37 ± 10.76**	**5.21**	**2.04**	**0.033**
[Mg]	19.39 ± 3.27	26.11 ± 4.29	−1.69	4	0.166
[Na]	**39.35 ± 3.04**	**1.28 ± 1.02**	**15.09**	**4**	**>0.001**
[Ni]	0.12 ± 0.00	0.07 ± 0.04	0.58	2	0.622
[P]	5.88 ± 0.12	5.92 ± 1.00	−0.07	2.06	0.9513
[Pb]	**0.55 ± 0.01**	**27.86 ± 3.99**	**−9.26**	**2**	**0.011**
[S]	17.45 ± 1.17	14.37 ± 2.39	0.26	4	0.809
[Si]	**840.30 ± 6.08**	**408.16 ± 86.66**	**5.29**	**2.02**	**0.033**
[Zn]	**0.26 ± 0.03**	**45.62 ± 6.25**	**−9.75**	**2**	**0.010**

Data are mean ($mg \cdot g^{-1}$) ± SD of three replicates; l.o.d = Limit of Detection. The last three columns report statistical results: bold letters indicate significance of differences between element content of control and contaminated *L. cruciata*.

values: Cu ($R = 0.63$, df = 3, $p = 0.26$), Fe ($R = 0.73$, df = 4, $p = 0.09$), Pb ($R = 0.72$, df = 4, $p = 0.11$) and Zn ($R = 0.72$, df = 4, $p = 0.11$). As for Cd, the inability to find a significant correlation with total sesquiterpenes should be explained by Control *L. cruciata* thalli being completely devoid of Cd.

Extract composition

A total of 98 and 84 compounds was detected in extracts from Control and Contaminated individuals, respectively (Table S3). Control and Contaminated *L. cruciata* shared 84 compounds, Control *L. cruciata* had 14 exclusive compounds, while Contaminated *L. cruciata* had no exclusive compounds (Table 4). In general, the chemical composition of Contaminated and Control *L. cruciata* extracts resembles in the percentage presence of each chemical class, except for sesquiterpenes (Fig. 2). Sesquiterpenes constituted 24.9% of Contaminated *L. cruciata* extract, which is more than twice that found in Control *L. cruciata* extract (11.98%), this difference is statistically significant (t-test = 152.91, df = 4, $p < 0.001$).

To delve into the differences in extracts' composition, a PCA was carried out considering plants' elements content and BVOCs profiles in the two studied populations. PCA first two dimensions explained 71.9% of total data variability: 54.8% and 17.1% by PC1 and PC2, respectively (Fig. 3, Figure S2). PCA biplot clearly separates Control and Contaminated individuals into two clusters following PC1, indicating marked diversity between Control and Contaminated *L. cruciata* volatile secondary metabolites profiles (Figure S3 shows contribution of each element to PC1). Sesquiterpenes were strongly associated with Contaminated *L. cruciata* (10-epi-α-eudesmol, germacrene-D, sesquisabinene hydrate, γ-cadinene, germacrene-B, nerolidol, T-muurolol). The correlation between total sesquiterpenes and heavy metals (Cd, Cu, Fe, Pb, Zn) were consequently tested and were significant and positive for Cu ($R = 0.98$, df = 3, $p = 0.003$), Fe ($R = 0.96$, df = 4, $p = 0.002$), Pb ($R = 0.98$, df = 4, $p = 0.001$) and Zn ($R = 0.98$, df = 4, $p = 0.001$). As for Cd, as stated above Control *L. cruciata* was completely devoid of Cd in its thalli. Increasing heavy metals in *L. cruciata* thalli, however, are not correlated with significant variations in F_v/F_m ($R = 0.66$, df = 4, $p = 0.16$). This means that photosynthetic efficiency of PSII is maintained at levels within the range of optimal photosynthesis, despite the presence of phytotoxic heavy metals within Contaminated *L. cruciata* thalli.

To explore at compound level resolution the correlations between BVOCs and heavy metals content in *L. cruciata*, we tested the correlations between Cd, Cu, Fe, Pb, and Zn levels in *L. cruciata* thalli and BVOCs produced by the liverwort to identify secondary metabolites with positive or negative responses to increasing concentrations of heavy metals in plant

Table 3. Variations in fluorescence parameters of *Lunularia cruciata* from control and contaminated populations.

				test statistics			
measurement	population	mean	variation %[a]	test statistic	df	*p*-value	ES[b]
F_0	Control	245.00	25.39%	$t = 2.85$	23	0.01	1.12 large
	Contaminated	307.20					
F_m	Control	862.10	39.88%	$t = 4.05$	23	>0.001	1.60 large
	Contaminated	1205.93					
F_v/F_m	Control	0.71	4.22%	$t = 3.46$	23	0.002	1.36 large
	Contaminated	0.74					
$F_v/2$	Control	305.55	47.07%	$t = 4.26$	23	>0.001	1.68 large
	Contaminated	449.37					
F_0/F_v	Control	0.40	−15.00%	$t = -3.28$	23	0.003	−1.30 large
	Contaminated	0.34					

F_0 = Minimum Fluorescence of 1 h Dark-Adapted Plants; F_m = Maximum Fluorescence After Application of a Saturating Light Pulse; F_v = Variable Fluorescence: Difference Between F_m and F_0; F_v/F_m = Photosystem II Maximum Quantum Yield, Calculated as $F_v/F_m = (F_m - F_0)/F_m$; $F_v/2$ = Plastoquinone Pool; F_0/F_v = Efficiency of Photosynthesis Water-Splitting Apparatus.

[a]% variation with respect to values measured on controls.

[b]Cohen's *d* effect size Hedge's Corrected for small samples (n < 50), ES values should be interpreted as: 0.2 or less suggests a small effect, ca. 0.5 indicates moderate effect, 0.8 or more signifies a large effect.

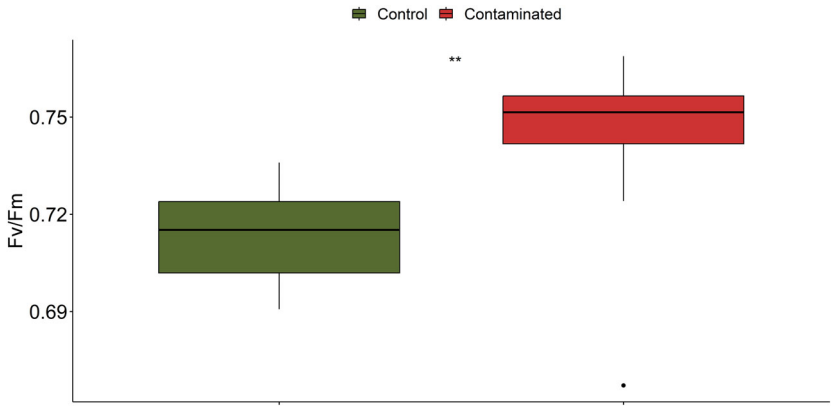

Fig. 1. Boxplots showing F_v/F_m in control and contaminated *Lunularia cruciata* thalli. Green and red boxes represent, respectively, control and contaminated values. Each boxplot reports 50% of measured values (inside the box), comprised between the first quartile value (lower side of the box) and third quartile value (upper side of the box); median is indicated by a black line inside the box, whiskers join the first and third quartiles with the lower and higher measured value, respectively (outliers are reported by black dots). *t*-test result is reported in the top left portion of the plot (asterisks indicate $*p < 0.05$; $**p < 0.01$; $***p < 0.001$).

Table 4. Relative abundance and number of compounds in each chemical class in extracts from control and contaminated populations of *Lunularia cruciata*.

	control		contaminated	
classes	%[a]	n[b]	%[a]	n[b]
Acids	2.53	1	1.93	1
Alcohols	0.29	2	0.14	1
Aldehydes	1.60	10	2.68	8
Ketones	6.15	3	5.59	2
Monoterpenes	1.54	14	0.99	8
Saturated Hydrocarbons	62.65	21	53.69	19
Sesquiterpenes	11.98	19	24.90	17
Unsaturated hydrocarbons	13.25	28	10.08	28

[a]Relative abundance of each chemical class in extracts.
[b]Number of compounds belonging to each chemical class.

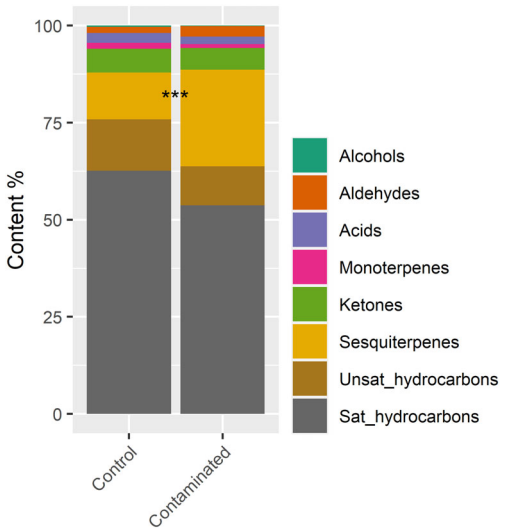

Fig. 2. Relative abundance of chemical classes. Stacked bar plots report relative abundance of each chemical class in control and contaminated individuals of *Lunularia cruciata* in different colours. Asterisks indicate $*P < 0.05$; $**P < 0.01$; $***P < 0.001$.

tissues (Fig. 4). Additional information on correlation methods, correlation coefficient, test statistics, DF and *p*-values can be found in Table S4.

DISCUSSION

Colonizing polluted post-mining environments is challenging for bryophytes. Bryophytes rely on diffusion from the surrounding environment for water and nutrients and, consequenly have poor control over the entry of pollutants into their tissues (Chakrabortty & Paratkar 2006; Basile *et al.* 2017; De Agostini *et al.* 2020b). In the present study, as expected, element profiles of *L. cruciata* clearly reflected soil geochemistry of the growing sites; Contaminated *L. cruciata* contains considerable amounts of soil pollutants in its thalli. Despite this, the presence of *L. cruciata* in this post-mining environment is stable and permanent as it produces dense and healthy carpets each year (is an annual species). In both Control and Contaminated sites, *L. cruciata* is present with comparable densities, with no stress symptoms of heavy metal exposure (Figure S1), such as leaf chlorosis, necrosis or abnormalities, or reduced biomass (Ghuge *et al.* 2023). Beside morphological uniformity, NDVI of *L. cruciata* highlighted how both Control and Contaminated plants can absorb adequate amounts of PAR for photosynthesis, resulting in healthy and vigorous populations (Chiocchio *et al.* 2022). To better understand if and how heavy metals affected *L. cruciata* use of light when growing on mining wastes, chlorophyll fluorescence was analysed. Photosynthesis is in fact immediately affected in presence of stresses, particularly in presence of heavy metals stress (Mallick & Mohn 2003). Chlorophyll fluorescence measurements also help to locate the primary mode of action of xenobiotics on photosystems (Mallick & Mohn 2003; Boisvert *et al.* 2007; Velikova *et al.* 2011) which, in both algae and vascular plants is generally photosystem II (PSII) (Mallick & Mohn 2003; Boisvert *et al.* 2007; Velikova *et al.* 2011; Bibbiani *et al.* 2018). In

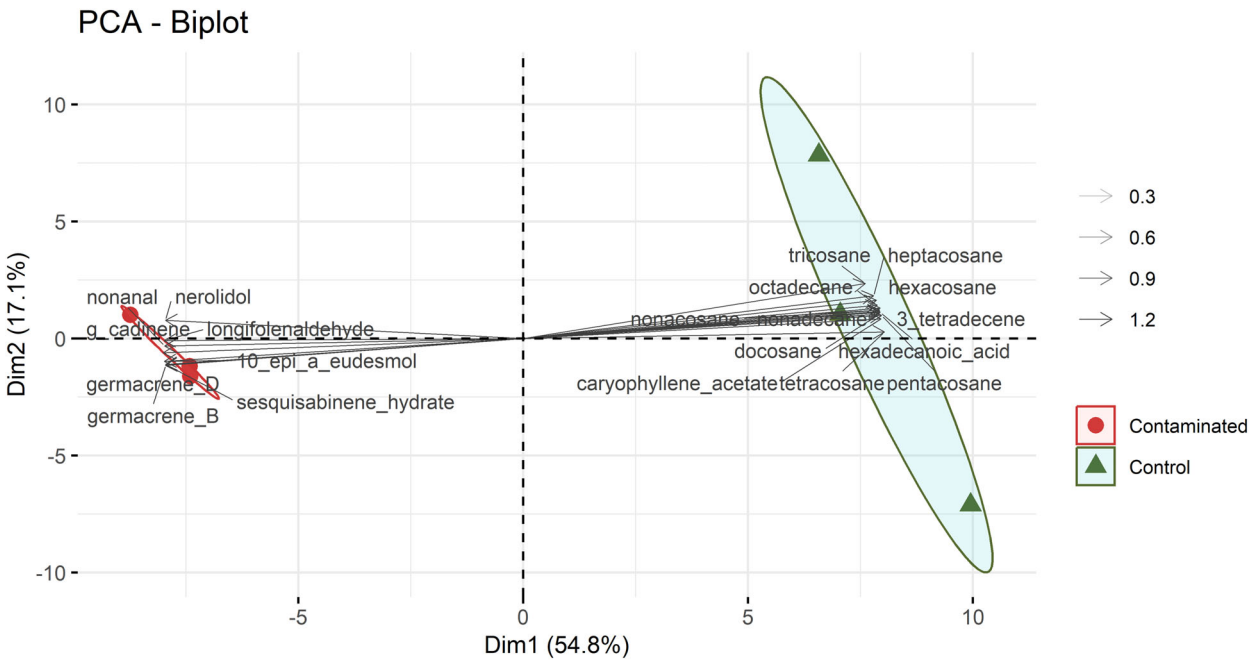

Fig. 3. PCA biplot. Green dots and red triangles indicate, respectively, control and contaminated individuals. 95% confidence ellipses are drawn around control and contaminated individuals. Variables are represented as arrows where length and opacity are proportional to their contribution to the PCA. Variables pointing in the same direction are directly proportional, while variables pointing in opposite directions are inversely proportional. Variables pointing towards clusters of individuals are highly representative of the features of that cluster. To improve readability of the plot, the 20 most contributing variables to PCA principal dimensions have been plotted.

the present study F_0, F_m, F_v/F_m, $F_v/_2$ and F_0/F_v were considered as indicative of the state and efficiency of PSII. The results show that, beside a negative effect on PSII antenna complex, electron flux from PSII to PSI and maximum quantum yield of PSII are conserved in Contaminated *L. cruciata*, indicating intact and efficient photosynthetic membranes of chloroplasts. Although increasing F_0 indicates that the transfer of excitation energy from PSII antenna complex to its reaction centre in Contaminated *L. cruciata* is negatively affected (Mallick & Mohn 2003), the plant is still able to maintain maximum quantum yield of PSII (F_v/F_m) at comparable levels to that of the Controls and unrelated to increasing heavy metals in thalli. Hence, both Control and Contaminated *L. cruciata* largely maintain photosynthesis levels considered optimal for bryophytes (López-Pozo *et al.* 2019). This is in stark contrast with the effects generally associated with heavy metal toxicity in plants and might be attributed to a well-preserved electron flux from PSII to photosystem I (PSI), as also witnessed by increased maximal fluorescence yield, enhanced plastoquinone pool and increased activity of the water-splitting apparatus (higher F_m, $F_v/2$ and F_0/F_v in Contaminated *L. cruciata*).

Volatile secondary metabolites of Contaminated and Control *L. cruciata* were largely similar, except for the sesquiterpene fraction, which doubled in Contaminated *L. cruciata* compared to controls. This difference suggests that the synthesis of specific protective secondary metabolites, particularly sesquiterpenes, is pivotal in preserving photosynthetic machinery in contaminated *L. cruciata*. Sesquiterpenes are volatile secondary metabolites belonging to the chemical class of VIs. VIs are known to be important in stress resistance, towards high light, extreme temperature, drought, oxidizing atmosphere, and heavy metals (Peñuelas & Munné-Bosch 2005; Vickers *et al.* 2009; Loreto *et al.* 2014b). VIs (both constitutive and induced) might counteract heavy metal stress by: (i) stabilizing hydrophobic interactions in membranes through their lipophilic nature, preserving their integrity and structure; and (ii) preventing oxidative damage by scavenging excess ROS thanks the presence of conjugated double bonds in VIs (Vickers *et al.* 2009; Velikova *et al.* 2011; Bibbiani *et al.* 2018).

In the present study, we framed enhanced sesquiterpenes in Contaminated *L. cruciata* within a VIs-based defence strategy allowing the plants to withstand heavy metals. The efficiency of the electron transport chain from PSII to PSI indicates healthy and efficient thylakoidal membranes in contaminated individuals (comparable to controls) attributable to the stabilizing and antioxidant properties of sesquiterpenes. To avoid inefficient light use and impaired photosynthesis is in fact crucial to cope with adverse environmental conditions and to prevent accumulation of ROS and exacerbate oxidative stress within the cell (Vickers *et al.* 2009). The literature on the role of VIs and sesquiterpenes in resistance to biotic (herbivory, pathogens) and abiotic (drought, heat, oxidative atmosphere) stresses and in adaptation to extreme environments in vascular plants is growing fast and the environmental role of these secondary metabolites is more and more sound (Kesselmeier & Staudt 1999; Rasmann *et al.* 2005; Vickers *et al.* 2009; Dicke & Baldwin 2010; Loreto & Schnitzler 2010; Rinnan *et al.* 2014). The present study provides an ecological study case in which sesquiterpenes are clearly associated with the presence of a liverwort in an extreme metalliferous environment. There was a significant positive correlation between increasing heavy metals (Cu, Fe, Pb and Zn) in *L. cruciata* thalli and total

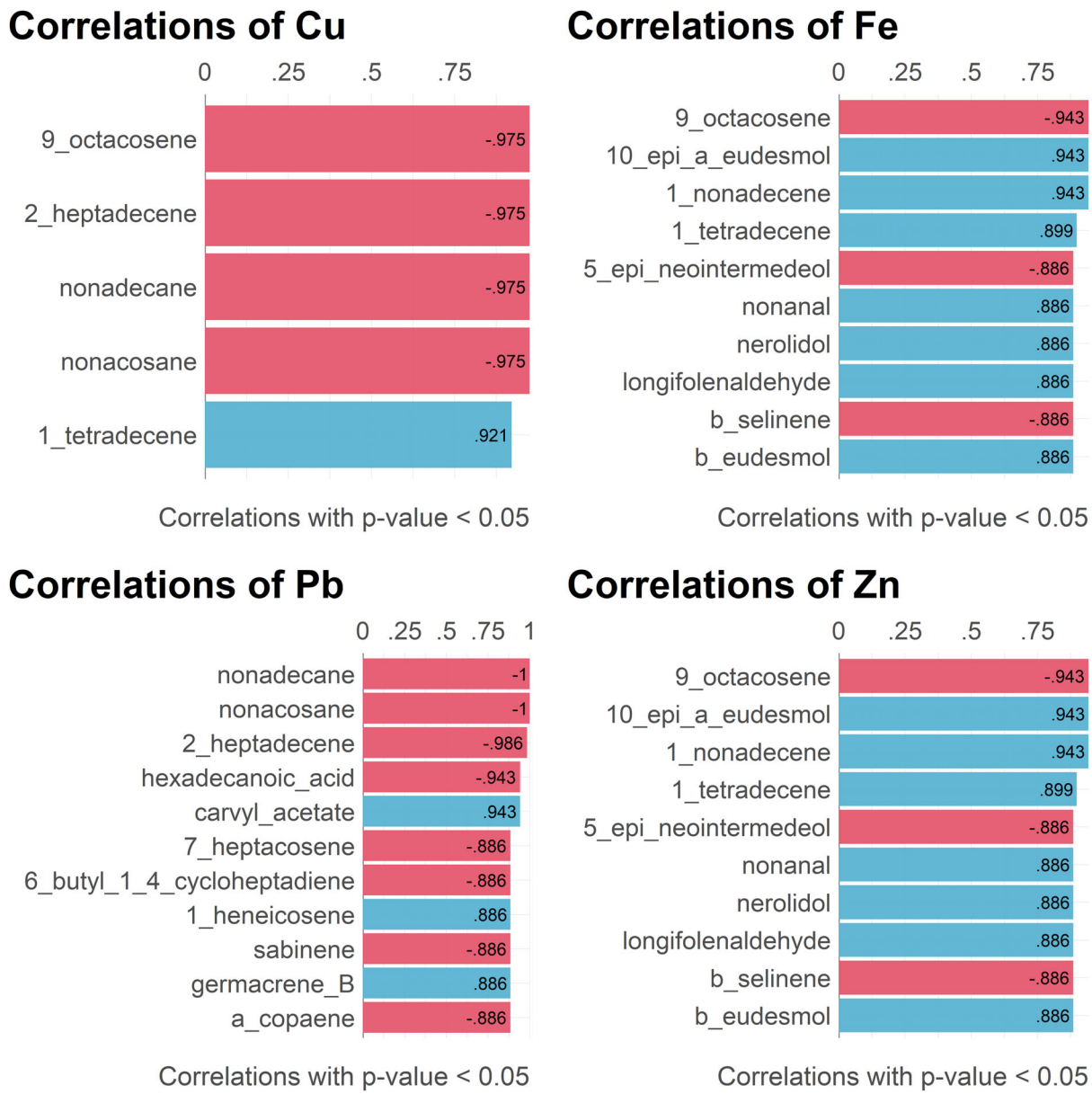

Fig. 4. Correlations between heavy metals in *Lunularia cruciata* thalli and chemical compounds in extracts. In the four panels are reported only the statistically significant correlations (correlation $p < 0.05$) between the concentration of each heavy metal measured in *L. cruciata* thalli and the compounds identified in *L. cruciata* extracts. Blue and red bars indicate positive and negative correlations, respectively.

sesquiterpenes fraction of its BVOCs. The VIs positively correlated with increasing heavy metals are 10-epi-α-eudesmol, germacrenes (B and D), sesquisabinene hydrate, γ-cadinene, nerolidol, T-muurolol, β-caryophyllene, and β-eudesmol, while non-isoprenic BVOCs also positively correlated with increasing heavy metals are nonanal, longifolenaldehyde, and pyran-5-one-2,2-dimethyl-7-isobutyl-2H-5H-pyrano. These compounds have been identified in liverworts and vascular plants in response to abiotic stresses such as salinity, cold, drought, and water deficit (more details and references in Table S5). Notably, this is the first study in which these compounds were associated to a wild liverwort population withstanding extreme heavy metal soil pollution.

Liverworts as *L. cruciata* can synthesize and store numerous and diverse isoprenoid secondary metabolites, unlike many bryophytes and land plants, because of the presence of both plant-typical and microbial-like genes for terpenoid biosynthesis and because of the presence of oil bodies (Chen *et al.* 2018a). This ability to synthesize and store a wide variety of VIs may have equipped the studied species with a readily available defensive strategy that may had resulted crucial in its ability to adapt to the metalliferous niche. The absence of exclusive compounds in Contaminated *L. cruciata* volatile profile suggests that *de novo* synthesis of specific compounds in response to the metalliferous environment is unlikely but the defensive BVOCs normally synthesized by *L. cruciata* also in

non-stressful conditions are enhanced when environmental heavy metals posed a threat to its survival.

We here propose a role of VIs, particularly sesquiterpenes, in mitigation of heavy metals adverse effects, by protecting *L. cruciata* photosynthetic membranes and so guaranteeing optimal photosynthesis and avoidance of oxidative stress from impaired photosynthesis, when inhabiting an extreme environment. Such an adaptive strategy might be related to the inherent ability of liverworts to synthesize and store a great variety of protective VIs. In conclusion, within this study new knowledge was gained on the role of VIs in non-vascular plants coping with adverse environmental conditions and environmental heavy metals.

AUTHOR CONTRIBUTIONS

ADA, PC, FSR, FG, CSA: Conceptualization; ADA, PC, FSR, FG, CSA: Project administration; ADA, PC, FSR, FS, DNT, FG, AV, CSA: Investigation and methodology; ADA, PC, CSA: Supervision; FG: Funding Acquisition; ADA, PC, AV, CSA: Resources; ADA: Data curation; ADA, PC, CSA: Validation; ADA, PC, CSA: Writing – original draft; ADA, PC, FSR, FS, CSO, DNT, FG, AC, AV, CSA: Writing – review and editing; ADA, PC, CSA: Visualization.

FUNDING INFORMATION

This research was funded by the "National Biodiversity Future Center (NBFC), National Recovery and Resilience Plan (NRRP), Mission 4 Component 2 Investment 1.4, Call for tender No. 3138 of 16 December 2021, rectified by Decree n.3175 of 18 December 2021 of the Italian Ministry of University and Research funded by the European Union, Next Generation EU, Project code CN_00000033.

SUPPORTING INFORMATION

Additional supporting information may be found online in the Supporting Information section at the end of the article.

Figure S1. *Lunularia cruciata* growing in control (panels A and B) and contaminated (panels C and D) sites.

Figure S2. Barplot of variable contribution to PC1 and PC2 referring to PCA reported in Fig. 3.

Figure S3. Barplot of variable contributions to PC1 referring to PCA reported in Fig. 3. Red and green boxes highlight whether each element mostly contributes to contaminated or control *Lunularia cruciata* cluster, respectively.

Table S1. Normalized diversity vegetation index (NDVI) values of *Lunularia cruciata* from control and contaminated population.

Table S2. Fluorescence parameters of *Lunularia cruciata* from control and contaminated population.

Table S3. Specialized metabolites detected in the extracts obtained from contaminated and control individuals of *Lunularia cruciata*.

Table S4. Significant correlations between HMs concentrations in *Lunularia cruciata* thalli and compounds in *Lunularia cruciata* extracts.

Table S5. Additional literature cases where the sesquiterpenes associated in the present study with contaminated *Lunularia cruciata* were described to be involved in stress responses.

REFERENCES

Adams R.P. (2017) *Identification of essential oil components by gas chromatography/mass spectrometry*, 5th edition. Texensis, TX, USA, Gruver.

Baker A.J.M., Ernst W.H.O., van der Ent A., Malaisse F., Ginocchio R. (2010) Metallophytes: the unique biological resource, its ecology and conservational status in Europe, central Africa and Latin America. In: Batty L.C., Hallberg K.B. (Eds), *Ecology of industrial pollution. Ecological reviews*. Cambridge University Press, Cambridge, UK, pp 7–40.

Basile A., Loppi S., Piscopo M., Paoli L., Vannini A., Monaci F., Sorbo S., Lentini M., Esposito S. (2017) The biological response chain to pollution: a case study from the "Italian Triangle of Death" assessed with the liverwort *Lunularia cruciata*. *Environmental Science and Pollution Research*, **24**, 26185–26193.

Beane S.J., Comber S.D.W., Rieuwerts J., Long P. (2016) Abandoned metal mines and their impact on receiving waters: a case study from Southwest England. *Chemosphere*, **153**, 294–306.

Bibbiani S., Colzi I., Taiti C., Guidi N.W., Papini A., Mancuso S., Gonnelli C. (2018) Smelling the metal: volatile organic compound emission under Zn excess in the mint *Tetradenia riparia*. *Plant Science*, **271**, 1–8.

Boisvert S., Joly D., Leclerc S., Govindachary S., Harnois J., Carpentier R. (2007) Inhibition of the oxygen-evolving complex of photosystem II and depletion of extrinsic polypeptides by nickel. *Biometals*, **20**, 879–889.

Campbell C., Kelly D.L., Smyth N., Lockhart N., Holyoak D.T., Long D. (2023) Investigation of the copper requirements of the metallophyte liverworts *Cephaloziella nicholsonii* Douin and *C. massalongoi* (Spruce) Müll.Frib. *Plants*, **12**, 2265.

Chakrabortty S., Paratkar G.T. (2006) Biomonitoring of trace element air pollution using mosses. *Aerosol and Air Quality Research*, **6**, 247–258.

Chen F., Ludwiczuk A., Wei G., Chen X., Crandall-Stotler B., Bowman J.L. (2018a) Terpenoid secondary metabolites in bryophytes: chemical diversity, biosynthesis and biological functions. *Critical Reviews in Plant Sciences*, **37**, 210–231.

Chen Y.E., Mao H.T., Ma J., Wu N., Zhang C.M., Su Y.Q., Zhang Z.W., Yuan M., Zhang H.Y., Zeng X.Y., Yuan S. (2018b) Biomonitoring chromium III or VI soluble pollution by moss chlorophyll fluorescence. *Chemosphere*, **194**, 220–228.

Chiocchio I., Barbaresi A., Barbanti L., Mandrone M., Poli F., Torreggiani D., Trenta M., Tassinari P. (2022) Effects of LED supplemental lighting on the growth and metabolomic profile of *Taxus baccata* cultivated in a smart greenhouse. *PLoS One*, **17**, e0266777.

De Agostini A., Caltagirone C., Caredda A., Cicatelli A., Cogoni A., Farci D., Guarino F., Garau A., Labra M., Lussu M., Piano D., Sanna C., Tommasi N., Vacca A., Cortis P. (2020a) Heavy metal tolerance of orchid populations growing on abandoned mine tailings: a case study in Sardinia Island (Italy). *Ecotoxicology and Environmental Safety*, **189**, 110018.

De Agostini A., Cogoni A., Cortis P., Vacca A., Becerril J.M., Hernández A., Esteban R. (2022) Heavy metal tolerance strategies in metallicolous and non-metallicolous populations of mosses: insights of γ+β-tocopherol regulatory role. *Environmental and Experimental Botany*, **194**, 104738.

De Agostini A., Cortis P., Cogoni A. (2020b) Monitoring of air pollution by moss bags around an oil refinery: a critical evaluation over 16 years. *Atmosphere*, **11**, 272.

De Giudici G., Medas D., Cidu R., Lattanzi P., Rigonat N., Frau I., Podda F., Marras P.A., Dore E., Frau F., Rimondi V., Runkel R.L., Wanty R.B., Kimball B. (2019) Assessment of origin and fate of contaminants along mining-affected Rio Montevecchio (SW Sardinia, Italy): a hydrologic-tracer and environmental mineralogy study. *Applied Geochemistry*, **109**, 104420.

Degola F., Sanità Di Toppi L., Petraglia A. (2022) Bryophytes: how to conquer an alien planet and live happily (ever after). *Journal of Experimental Botany*, **73**, 4267–4272.

Dicke M., Baldwin I.T. (2010) The evolutionary context for herbivore-induced plant volatiles: beyond the "cry for help". *Trends in Plant Science*, **15**, 167–175.

Ghuge S.A., Nikalje G.C., Kadam U.S., Suprasanna P., Hong J.C. (2023) Comprehensive mechanisms of heavy metal toxicity in plants, detoxification, and remediation. *Journal of Hazardous Materials*, **450**, 131039.

Hodson M.J. (2012) Metal toxicity and tolerance in plants. *The Biochemist*, **34**, 28–32.

IUSS Working Group WRB (2022) *World Reference Base for soil resources. International soil classification system for naming soils and creating legends for soil maps*, 4th edition. International Union of Soil Sciences (IUSS), Vienna, Austria.

Karakaya M.Ç., Karakaya N., Küpeli Ş., Karadağ M.M., Kirmaci M. (2015) Potential bioaccumulator mosses around massive sulfide deposits in the vicinity of the Giresun area, northeast Turkey. *CLEAN - Soil, Air, Water*, **43**, 27–37.

Kesselmeier J., Staudt M. (1999) Biogenic volatile organic compounds (VOC): an overview on emission, physiology and ecology. *Journal of Atmospheric Chemistry*, **33**, 23–88.

López-Pozo M., Flexas J., Gulías J., Carriquí M., Nadal M., Perera-Castro A.V., Clemente-Moreno M.J., Gago J., Núñez-Olivera E., Martínez-Abaigar J., Hernández A., Artetxe U., Bentley J., Farrant J.M., Verhoeven A., García-Plazaola J.I., Fernández-Marín B. (2019) A field portable method for the semi-quantitative estimation of dehydration tolerance of photosynthetic tissues across distantly related land plants. *Physiologia Plantarum*, **167**, 540–555.

Li F.W., Nishiyama T., Waller M., Frangedakis E., Keller J., Li Z., Fernandez-Pozo N., Barker M.S., Bennett T., Blázquez M.A., Cheng S., Cuming A.C., de Vries J., de Vries S., Delaux P.M., Diop I.S., Harrison C.J., Hauser D., Hernández-García J., Kirbis A., Meeks J.C., Monte I., Mutte S.K., Neubauer A., Quandt D., Robison T., Shimamura M., Rensing S.A., Villarreal J.C., Weijers D., Wicke S., Wong G.K.S., Sakakibara K., Szövényi P. (2020) *Anthoceros* genomes illuminate the origin of land plants and the unique biology of hornworts. *Nature Plants*, **6**, 259–272.

Liang L., Tang H., Deng Z., Liu Y., Chen X., Wang H. (2018) Ag nanoparticles inhibit the growth of the bryophyte, *Physcomitrella patens*. *Ecotoxicology and Environmental Safety*, **164**, 739–748.

Loreto F., Dicke M., Schnitzler J.P., Turlings T.C.J. (2014a) Plant volatiles and the environment. *Plant, Cell and Environment*, **37**, 1905–1908.

Loreto F., Pollastri S., Fineschi S., Velikova V. (2014b) Volatile isoprenoids and their importance for protection against environmental constraints in the Mediterranean area. *Environmental and Experimental Botany*, **103**, 99–106.

Loreto F., Schnitzler J.P. (2010) Abiotic stresses and induced BVOCs. *Trends in Plant Science*, **15**, 154–166.

Mallick N., Mohn F.H. (2003) Use of chlorophyll fluorescence in metal-stress research: a case study with the green microalga *Scenedesmus*. *Ecotoxicology and Environmental Safety*, **55**, 64–69.

Peñuelas J., Llusià J. (2004) Plant VOC emissions: making use of the unavoidable. *Trends in Ecology & Evolution*, **19**, 402–404.

Peñuelas J., Munné-Bosch S. (2005) Isoprenoids: an evolutionary pool for photoprotection. *Trends in Plant Science*, **10**, 166–169.

R Core Team (2022). *R: A language and environment for statistical computing*. Vienna, Austria: R Foundation for Statistical Computing. URL https://www.R-project.org/

Rascio N., Navari-Izzo F. (2011) Heavy metal hyperaccumulating plants: how and why do they do it? And what makes them so interesting? *Plant Science*, **180**, 169–181.

Rasmann S., Kollner T.G., Degenhardt J., Hiltpold I., Toepfer S., Kuhlmann U., Gershenzon J., Turlings T.C.J. (2005) Recruitment of entomopathogenic nematodes by insect-damaged maize roots. *Nature*, **434**, 732–737.

Rinnan R., Steinke M., Mcgenity T., Loreto F. (2014) Plant volatiles in extreme terrestrial and marine environments. *Plant, Cell and Environment*, **37**, 1776–1789.

Robustelli della Cuna F.S., Calevo J., Bari E., Giovannini A., Boselli C., Tava A. (2019) Characterization and antioxidant activity of essential oil of four sympatric orchid species. *Molecules*, **24**, 3878.

Robustelli della Cuna F.S., Cortis P., Esposito F., De Agostini A., Sottani C., Sanna C. (2022) Chemical composition of essential oil from four sympatric orchids in NW-Italy. *Plants*, **11**, 826.

Rodríguez-Eugenio N., McLaughlin M., Pennock D. (2018) Soil pollution: a hidden reality FAO report.

Schoeneberger P.J., Wysocki D.A., Benham E.C., Soil Survey Staff (2012) *Field book for describing and sampling soils, version 3.0*. Lincoln, NE, USA: Natural Resources Conservation Service, National Soil Survey Center.

Singh M., Kumar J., Singh S., Singh V.P., Prasad S.M., Singh M. (2015) Adaptation strategies of plants against heavy metal toxicity: a short review. *Biochemistry & Pharmacology: Open Access*, **4**, 2167-0501.

Smith, A.J.E. (1990) *The The Liverworts of Britain & Ireland*. Cambridge, UK: Cambridge University Press, pp. 378.

Stein S.E. (2000) NIST/EPA/NIH Mass Spectral Database, Version 2.1.

Thomas J. (2003) *NIST standard reference materials catalog 2003, special publication (NIST SP)*. National Institute of Standards and Technology, Gaithersburg, MD, USA.

Varrica D., Tamburo E., Milia N., Vallascas E., Cortimiglia V., De Giudici G., Dongarrà G., Sanna E., Monna F., Losno R. (2014) Metals and metalloids in hair samples of children living near the abandoned mine sites of Sulcis-Inglesiente (Sardinia, Italy). *Environmental Research*, **134**, 366–374.

Velikova V., Tsonev T., Loreto F., Centritto M. (2011) Changes in photosynthesis, mesophyll conductance to CO_2, and isoprenoid emissions in *Populus nigra* plants exposed to excess nickel. *Environmental Pollution*, **159**, 1058–1066.

Vickers C.E., Gershenzon J., Lerdau M.T., Loreto F. (2009) A unified mechanism of action for volatile isoprenoids in plant abiotic stress. *Nature Chemical Biology*, **5**, 283–291.